

Application of parametric methods of power spectrum estimation in passive sonar signals classification

J. Schmidt ⁽¹⁾, R. Salamon ⁽²⁾

Technical University of Gdansk, Acoustics Department, Narutowicza 11/12, 80-952 Gdansk, POLAND

⁽¹⁾ e-mail: yanie@eti.pg.gda.pl, ⁽²⁾ e-mail: salamon@pg.gda.pl

The paper presents the signals classification method based on the parametric spectral analysis as applied to the passive sonar. The system's structure is discussed special emphasis is given to the procedure of features selection in which true poles are chosen. Attached are results of tests carried out to evaluate the applicability of parametric methods of spectral estimation for the purpose of creating acoustic portraits and their classification.

1. Introduction

The system of passive sonar usually consists of two subsystems i.e. detection and classification subsystems as depicted in Fig.1.

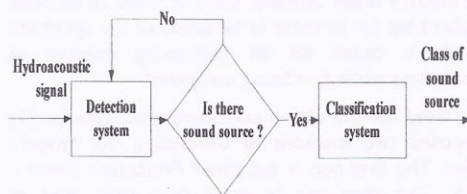


Fig.1. The system of passive sonar.

The detection subsystem's task is to detect a sound source, if present in a certain water region. This is done by processing of received hydroacoustic signal. The subsystem is the core of the entire system. Its operation makes it possible for the classification sub-system to perform its tasks [7].

The classification subsystem defines the type of a detected sound source using a databank of acoustic portraits. Its input receives the hydroacoustic signal supplied by the detection subsystem.

This paper presents the application of passive sonar signals classification based on parametric spectral analysis whose structure is shown in Fig 2.

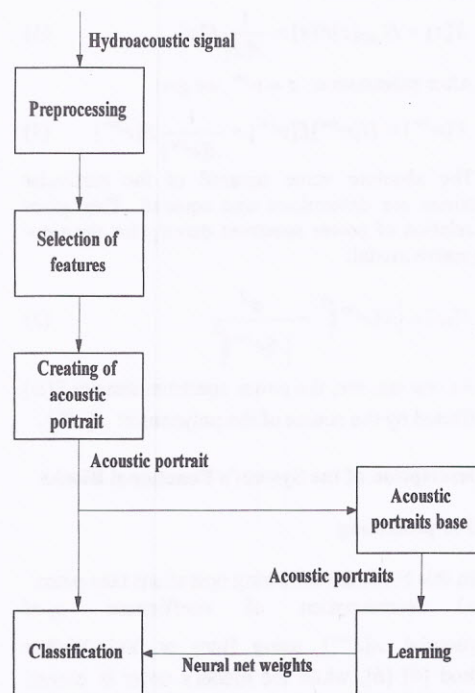


Fig.2. Diagram of the classification system of the passive sonar.

2. Parametric Methods of Spectral Analysis Based on Autoregression Process

Samples of the signal $u[n]$ being received are used to denote the time series $x[n], x[n-1], \dots, x[n-N]$ fulfilling the difference equation:

$$x[n] = -\sum_{k=1}^N a_k u[n-k] + e[n], \quad (1)$$

where a_1, \dots, a_N are coefficients of autoregression. These are determined using various methods based on prediction error power minimisation $e[n]$ expressed with a white noise of mean zero value and variance σ^2 .

Autoregression of order N is obtained as output signal $x[n]$ of a filter with a white noise applied to its input.

After transformation of both sides of the equation (1), the outcome is a transmittance of the filter, which models the autoregression process:

$$H_{AR}[z] = \frac{U[z]}{E[z]} = \frac{1}{1 + \sum_{k=1}^N a_k z^{-k}} = \frac{1}{A[z]}, \quad (2)$$

where $U[z]$ and $E[z]$ are Z -transforms of sequence $x[n]$ and $e[n]$ and

$$X[z] = H_{AR}[z]E[z] = \frac{1}{A[z]}E[z]. \quad (3)$$

After substitution: $z = e^{j\omega}$ we get:

$$X[e^{j\omega}] = H[e^{j\omega}]E[e^{j\omega}] = \frac{1}{A[e^{j\omega}]}E[e^{j\omega}] \quad (4)$$

The absolute value squared of the particular functions are determined and squared. This gives the relation of power spectrum density for the autoregressive model:

$$S[\omega] = |X[e^{j\omega}]|^2 = \frac{\sigma^2}{|A[e^{j\omega}]|^2} \quad (5)$$

As one can see, the power spectrum density $S[\omega]$ is affected by the course of the polynomial $A[e^{j\omega}]$.

3. Description of the System's Functional Blocks

3.1 Pre-processing

In this block the following operations take place:

a) determination of coefficients a_k of polynomial $A[e^{j\omega}]$ using Burg or Yule-Walker method [4] [6], while the model's order is chosen using Akaike information criterion [1],

b) solution of the equation:

$$A[z] = 1 + \sum_{k=1}^N a_k z^{-k} = 0 \quad (6)$$

to identify roots z_k of polynomial $A[z]$ ($S[\omega_k]$ poles) using Laguerre method.

In the process of spectral estimation using parametric methods, the critical problem lies in the choice of the right order of the model. When the chosen order of the model is too small, it makes the spectrum too flattened. If, on the other hand, the order accepted is too big, the resulting spectrum's resolution will be increased, however, containing false poles. This causes a general statistical instability.

For data with no noise, the estimates of the model's order make the resulting spectrum acceptable, if the number of the available data is not too small [1]. For data with strong noise, however, the choice of the model's order is usually insufficient to analyse the spectrum's details [5].

For the same estimate of the model's order, various models' orders are obtained, depending on the spectral estimation method applied. Almost all estimators of a model's order are based on prediction error power. The prediction error power being computed, either diminishes or stays flat for an increasing model's order. This applies to all spectral estimation methods for the autoregressive model. Controlling the process of diminishing the prediction error power cannot in itself be used to choose the model's order. Another thing that has to be done is checking the increase in variation of the spectrum which is based on an increasing number of parameters while it is being computed.

Based on the above considerations, Akaike [1] proposed two methods of estimating the model's order. The first one is the *Final Prediction Error - FPE*. The other one is most frequently used in practice the *Akaike Information Criterion - AIC* in which the order of model AR is estimated through minimization in relation to k of the following expression (Fig. 3):

$$AIC(k) = N_S \ln \hat{\rho}_k + 2k, \quad (7)$$

where $\hat{\rho}_k$ is the computed variance of white noise (prediction error power) for a k order of the autoregressive model, and N_S denotes the number of samples of the signal being analysed.

In the relation (7), the growing component $2k$ is interpreted as a punishment for adopting an order of the autoregressive model at a level that's too high.

Although the AIC method is not a consistent estimator, still for a big number of data the resulting order of the model is more accurate than that for FPE [2].

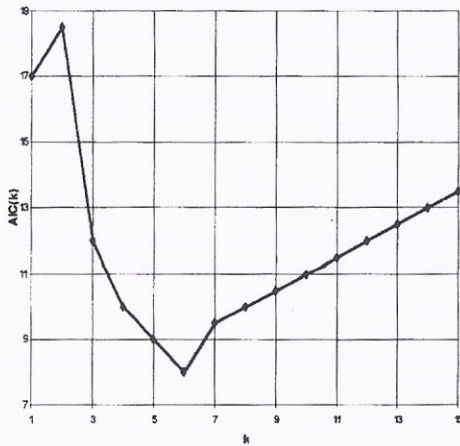


Fig. 3. Example of a chart of Akaike information criterion.

3.2 Selection of Features

Features are selected within the process of selecting "true poles" and searching of its frequencies.

The term true poles is used for those poles [3] which form peaks on the chart of power spectrum density (resonant peaks), while extra poles are poles responsible for an equiripple approximation of the flat noise spectrum.

As an example, for signal: $y(n) = \sin(2\pi f_1 \Delta t n) + \sin(2\pi f_2 \Delta t n) + e(n)$,

where $f_1 = 30$ [Hz], $f_2 = 77$ [Hz], $\Delta t = \frac{1}{N}$, $\sigma^2 = 0.05$,

with the assumed AR model order equal to 10, the chart of the poles has a form shown in Fig. 4.

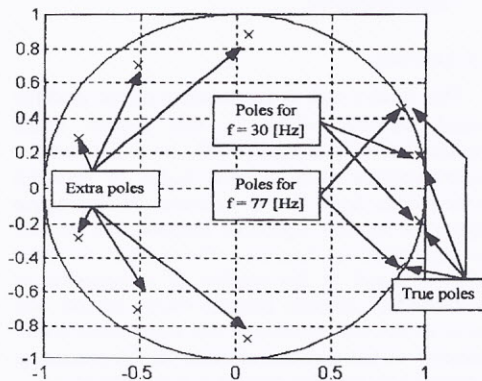


Fig. 4. Chart of poles.

In the procedure of selecting the "true poles", the area between the unit circle and the selection

circle describing the module indicator, forms a selection ring. By changing the radius of the selection circle, we either accept or reject the poles, as illustrated in Fig. 5.

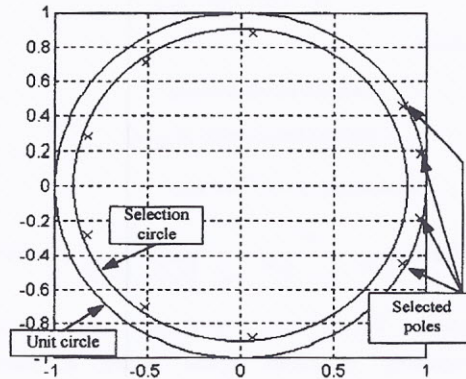


Fig. 5. Chart illustrating the procedure of "true poles" selection.

When choosing the "true poles", we have to bear the following in mind [3]:

- for signals with a high SNR, extra poles are located far from the unit circle towards its centre, and because of this they do not affect the spectrum.
- in a case of a diminishing SNR, the radii (modules) of true poles are diminishing; this continues until the radii are equal to the radii of extra poles.
- assuming a stable SNR, an increase in the AR model order causes an increase in the resolution of the spectrum being estimated, although in practice excessive increasing of the order makes the extra poles near the true poles, at which point false peaks can be observed in the spectrum.

For "true poles" that were selected in point a), we search for corresponding frequencies by determining ω_k from the relation $z_k = e^{j\omega_k}$, with

$$f_k = \frac{\omega_k}{2\pi} \quad (8)$$

3.3 Creating an Acoustic Portrait

For the determined frequencies, values of spectral lines are determined based on the poles given by the block "data selection". This is done through the geometrical method of determining the chart of power spectrum density.

Assuming that AR model transmittance has the form:

$$H_{AR}[z] = \frac{\sigma^2}{(z - z_1) \cdots (z - z_n)} \quad (9)$$

where

σ^2 - variance of white noise

z_n - transmittance poles $H_{AR}[z]$

Substituting $z = e^{j\omega}$ we get:

$$H_{AR}[\omega] = \frac{\sigma^2}{(e^{j\omega_k} - z_1) \cdots (e^{j\omega_k} - z_n)} = \frac{\sigma^2}{(\overline{N_1 L}) \cdots (\overline{N_n L})} \quad (10)$$

where $\overline{N_i L} = e^{j\omega_k} - z_i$, $i=1, \dots, n$ are vectors beginning at points z_i and ending at point $L = e^{j\omega_k}$ located in the unit circle.

N - number of all poles (order of AR model)

The appropriate power spectrum density relation has this form:

$$S[\omega_k] = |X[e^{j\omega_k}]|^2 = \left[\frac{\sigma^2}{(\overline{N_1 L}) \cdots (\overline{N_n L})} \right]^2 \quad (11)$$

The procedure is illustrated in Fig. 6.

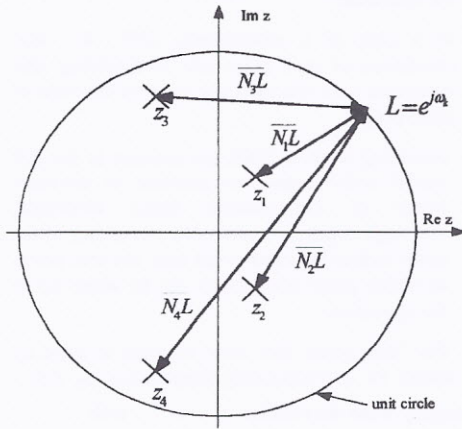


Fig. 6. Geometric method of determining the chart of power spectrum density for $N=4$.

The frequencies and the matching values of spectral lines constitute a so called primary acoustic portrait P_F of a sound source:

$$P_F = [f_1 \ A_1 \ f_2 \ A_2 \ \dots \ f_n \ A_n]^T$$

Based on the sound source's primary acoustic portrait, a secondary acoustic portrait is made taking into account the following :

- changes in sound source's speed (frequency of spectral lines)

$$f_{12} = \frac{f_2}{f_1}, \quad f_{1N} = \frac{f_N}{f_1}$$

- changes in the distance between sound source and hydrophone (value of spectral line)

$$A_{12} = \frac{A_2}{A_1}, \quad A_{1N} = \frac{A_N}{A_1}$$

These result in the secondary acoustic portrait P_S of the form:

$$P_S = [f_{12} \ A_{12} \ \dots \ f_{1N} \ A_{1N}]^T$$

3.4. Acoustic Portraits Base

This block is responsible for managing a base of acoustic portraits by enabling operations, such as:

- starting a new base and accepting its file as the file of the current base of acoustic portraits,
- adding the existing base file and accepting it as the file of the current acoustic portraits base,
- adding the acoustic portrait formed to the current acoustic portraits base,
- deleting an acoustic portrait of the current acoustic portraits base,
- displaying the contents of the current acoustic portraits base,
- export of secondary acoustic portraits contained in the current acoustic portraits base to the learning file in the SNNS 4.1 neural networks simulator.

3.5. Learning

This block's task is the learning of the artificial neural network, which in this system fulfils the function of a classifier [8]. It is a two-layer neural network with 6 input nodes, 4 neurones in the hidden layer and 3 neurones in the output layer. The unipolar sigmoidal function was adopted as the activation function. The number of input nodes is equal to the number of components of the secondary acoustic portrait whose number was set as 6. The consequence of this assumption is a limitation of the number of lines in the process of generating an acoustic portrait to 4 spectral lines.

Neural network learning is carried out off-line, because the procedure of learning is usually preceded with a long-lasting process of registering hydroacoustic signals which match the particular

types of sound sources. In the neural network learning process, secondary acoustic portraits are used.

The SNNS 4.1 (Stuttgart Neural Network Simulator) was chosen as the neural network learning programme, controlled by the Linux operating system.

3.6. Classification

The classification block placed highest within the classification subsystem hierarchy (Fig. 2), uses the results obtained in the preceding blocks of the system.

The inputs of a neural network after learning receive components of the secondary acoustic portrait of a sound source, so that after the computations the decision can be made based on the network's output values whether the sound source should be assigned to one of the classes or whether its membership in any of the classes should be excluded.

By assuming a continuous activation function, output signals of neurons assume continuous values from the range [0,1] instead of binary values where 1 would match an assigned class. Therefore, the process of sound source assignment (based on its acoustic portrait) to a certain class is carried out in two-stages. In the first stage, the values of output neurones are checked (levels of activation) to see if they have exceeded the value of the assumed threshold (set at 0.5). If this is not met, a decision is made that the signal source cannot be assigned to any of the class; if the outcome is contrary it is checked to what extent the output neuron with the highest value exceeds the others. If the difference is big enough (up to 0.15), the source signal is assigned a class for which the output neuron was adopting the highest value, otherwise the interpreter gives a result which is that the source signal has not been assigned to any of the classes.

The above interpreter is based on the assumption that no classification is better than a wrong classification.

4. Tests

To determine how useful the components of a secondary acoustic portrait are for classification (learning) purposes, obtained using Yule-Walker (Y-W) and Burg methods, tests were conducted for various values of amplitudes.

The generated signal's spectrum contained four harmonic lines (the maximal number accepted in the course of setting up an acoustic portrait).

Next, acoustic portraits matching the signal were designated.

Signal 1:

$$y(n) = A_1 \sin(2\pi f_1 \Delta t n) + A_2 \sin(2\pi f_2 \Delta t n) + A_3 \sin(2\pi f_3 \Delta t n) + A_4 \sin(2\pi f_4 \Delta t n) + e(n)$$

where

$$\begin{aligned} f_1 &= 30 \text{ [Hz]}, & f_2 &= 60 \text{ [Hz]}, \\ f_3 &= 90 \text{ [Hz]}, & f_4 &= 120 \text{ [Hz]} \end{aligned}$$

$$A_1 = 1, A_2 = 0.5, A_3 = 0.25, A_4 = 0.125$$

$$\Delta t = \frac{1}{N} = \frac{1}{1024},$$

vectors of secondary acoustic portraits were determined for several different noise values:

σ^2	Method	Vector P_s
0.01	Y-W	[2.00 0.95 3.00 0.86 4.03 0.79]
	Burg	[2.00 1.13 3.00 1.00 4.00 0.86]
0.05	Y-W	[2.00 0.93 3.00 0.84 4.00 0.77]
	Burg	[2.00 1.09 3.00 0.96 4.03 0.83]
0.25	Y-W	[2.00 0.91 3.03 0.82 4.03 0.77]
	Burg	[2.00 1.03 3.03 0.89 4.03 0.79]

For signal 2 whose form is like that of signal 1, however:

$$A_1 = 1, A_2 = 0.2, A_3 = 0.6, A_4 = 0.8$$

vectors of secondary acoustic portraits were determined in a similar way:

σ^2	Method	Vector P_s
0.01	Y-W	[1.97 0.80 3.00 0.99 4.09 1.01]
	Burg	[2.00 0.95 3.00 1.08 4.00 1.06]
0.05	Y-W	[2.00 0.81 3.00 0.98 4.00 1.01]
	Burg	[2.00 0.88 3.00 1.05 4.00 1.04]
0.25	Y-W	[2.00 0.79 3.00 0.97 4.00 0.98]
	Burg	[2.00 0.91 3.00 1.05 4.00 1.05]

For signal 3 whose form is like that of signal 1, however:

$$A_1 = 1, A_2 = 0.7, A_3 = 0.4, A_4 = 0.1$$

vectors of secondary acoustic portraits are as follows:

σ^2	Method	Vector P_s
0.01	Y-W	[2.01 1.01 3.00 0.93 4.03 0.76]
	Burg	[2.00 1.17 3.00 0.96 4.03 0.85]
0.05	Y-W	[2.00 1.00 3.00 0.91 4.07 0.75]
	Burg	[2.00 1.10 3.00 0.99 4.03 0.79]
0.25	Y-W	[2.00 0.97 3.00 0.89 4.03 0.76]
	Burg	[2.00 0.98 3.03 0.89 4.03 0.77]

Following an observation of charts of power spectrum density and based on the above results, it was found that Burg method gives a high-resolution spectrum, however, the general character of values of harmonic amplitudes is strongly distorted. In addition, there is a big variance among the values of components of the secondary acoustic portrait for different noise values. As an example, for signal 1 component f_{14} determined using Burg method has a spread of 0.7, while Yule-Walker has a spread of 0.02.

For Yule-Walker method, spectrum resolution is worse, yet it maintains the values of amplitudes of the particular harmonics, which is one of the fundamental advantages of the spectral estimation method. Its results are used to create an acoustic portrait.

To test the classifier, we used signals generated earlier on, i.e. signal 1, signal 2 and signal 3. We also assumed that class 1 will be represented by signal 1, class 2 by signal 2, and class 3 by signal 3.

Secondary acoustic portraits obtained for signals of $\sigma^2=0.01$ and $\sigma^2=0.25$ were accepted as learning patterns, while portraits obtained for signals $\sigma^2=0.05$ were accepted as testing patterns. All secondary acoustic portraits used for testing purposes were obtained through the application of Yule-Walker method as a spectral estimation method.

The results of the classification include the values of outputs of the neural network and the decision made by the interpreter.

Signal		Results of Classification			
No.	σ^2	Output class 1	Output class 2	Output class 3	Interpret. decision
		[%]	[%]	[%]	
1	0.05	90.81	4.68	11.08	1
2	0.05	9.45	88.48	12.06	2
3	0.05	9.87	10.34	89.85	3

All the obtained results meet the expected results.

5. Conclusion

The use of parametric spectral estimation in classification systems to determine acoustic portraits components, and next to classify these, is an alternative approach to the process of feature selection. The approach was based on a selection of true poles as opposed to solutions that are based on power spectrum estimation.

Since acoustic portraits are made on the basis of values of amplitudes and frequencies of the particular harmonics, Burg algorithm was rejected, because it does not maintain the amplitude values of the particular harmonics, although it does help to achieve high spectral resolution. For the purposes of the classification system, the Yule-Walker algorithm was accepted. It gives high resolution provided long data sequences are used. This particular condition is met in the case of passive sonar signal classification. Based on the results obtained, it seems worthwhile to examine algorithms, which will provide a higher resolution and maintain amplitude values for signals of a small SNR.

The classification results, when a neural network is used as the classifier, depend on the learning of this network. The tests confirmed the usefulness of secondary acoustic portraits as obtained in parametric spectral estimation for classification purposes.

6. References

- [1]. H. Akaike, A new look at the statistical model identification, IEEE Trans. On Automatic Control, Vol. AC19, pp. 716-723, (1974).
- [2]. R.L. Kashyap, Inconsistency of the AIC rule for estimating the order of autoregressive models, IEEE Trans. On Automatic Control, Vol. AC25, pp. 996-998, (1980).
- [3]. S.M. Kay, The effects of noise on the autoregressive spectral estimator, IEEE Trans. on ASSP, Vol. 27, No. 5, pp. 478-485, (1979).
- [4]. S.M. Kay, *Modern Spectral Estimation - Theory and Application*, N.J., Prentice-Hall, Englewood Cliffs, 1988, ch. 7.
- [5]. T.E. Landers, R.T. Lacoss, Some geophysical applications of autoregressive spectral estimates, IEEE Trans. Geosci. Electron., Vol. GE15, pp. 25-32, (1977).
- [6]. S.L. Marple Jr, *Digital Spectral Analysis*, N.J., Prentice-Hall, Englewood Cliffs, 1987, ch. 8.
- [7]. R. Salamon, Detection and positioning of target in passive sonars, XLIV OSA, Gdańsk-Jastrzębia Góra, pp.103-112, (1997).
- [8]. J.M. Zurada, *Introduction to Artificial Neural Systems*, West Publishing Company, St. Paul., 1992.